

# Image-based left ventricular shape analysis for sudden cardiac death risk stratification



Fijoy Vadakkumpadan, PhD, \* Natalia Trayanova, PhD, FHRS, \* Katherine C. Wu, MD<sup>†</sup>

From the \*Department of Biomedical Engineering, Institute for Computational Medicine, Johns Hopkins University, Baltimore, Maryland, and <sup>†</sup>Division of Cardiology, Department of Medicine, Johns Hopkins Medical Institutions, Baltimore, Maryland.

**BACKGROUND** Low left ventricular ejection fraction (LVEF), the main criterion used in the current clinical practice to stratify sudden cardiac death (SCD) risk, has low sensitivity and specificity.

**OBJECTIVE** To uncover indices of left ventricular (LV) shape that differ between patients with a high risk of SCD and those with a low risk.

**METHODS** By using clinical cardiac magnetic resonance imaging and computational anatomy tools, a novel computational framework to compare 3-dimensional LV endocardial surface curvedness, wall thickness, and relative wall thickness between patient groups was implemented. The framework was applied to cardiac magnetic resonance data of 61 patients with ischemic cardiomyopathy who were selected for prophylactic implantable cardioverter-defibrillator treatment on the basis of reduced LVEF. The patients were classified by outcome: group 0 had no events; group 1, arrhythmic events; and group 2, heart failure events. Segmental differences in LV shape were assessed.

**RESULTS** Global LV volumes and mass were similar among groups. Compared with patients with no events, patients in groups 1 and 2 had lower mean shape metrics in all coronary artery regions, with statistical significance in 9 comparisons, reflecting wall thinning and stretching/flattening.

**CONCLUSION** In patients with ischemic cardiomyopathy and low LVEF, there exist quantifiable differences in 3-dimensional endocardial surface curvedness, LV wall thickness, and LV relative wall thickness between those with no clinical events and those with arrhythmic or heart failure outcomes, reflecting adverse LV remodeling. This retrospective study is a proof of concept to demonstrate that regional LV remodeling indices have the potential to improve the personalized risk assessment for SCD.

**KEYWORDS** Sudden cardiac death; Cardiac magnetic resonance imaging; Computational anatomy; Shape analysis; Risk stratification; Implantable cardioverter-defibrillator

**ABBREVIATIONS** **2D** = 2-dimensional; **3D** = 3-dimensional; **AHA** = American Heart Association; **CMR** = cardiac magnetic resonance; **HF** = heart failure; **ICD** = implantable cardioverter-defibrillator; **LAD** = left anterior descending; **LV** = left ventricular; **LVEF** = left ventricular ejection fraction; **RWT** = relative wall thickness; **SAD** = sudden arrhythmic death; **SCD** = sudden cardiac death; **TEI** = transmural extent of the infarct; **WT** = wall thickness

(Heart Rhythm 2014;11:1693–1700) © 2014 Heart Rhythm Society. All rights reserved.

## Introduction

Sudden cardiac death (SCD) is a major health problem worldwide, affecting hundreds of thousands of persons annually in the United States alone.<sup>1</sup> As the survival rate of SCD is very small, it is of paramount importance to identify patients at risk and give them prophylactic treatment. It is also crucial that the patient identification method is specific, as implantable cardioverter-defibrillator (ICD) therapy, the most widespread preventive care for SCD, is costly and associated with serious risks.<sup>1</sup> However, the patient

selection criterion used in the current clinical practice, namely, left ventricular ejection fraction (LVEF)  $\leq 35\%$ , has low sensitivity and specificity.<sup>2</sup> Although numerous alternatives to SCD risk stratification have been proposed, the optimal approach remains unknown.<sup>3</sup>

It has been known for decades that cardiomyopathies are associated with adverse remodeling of left ventricular (LV) geometry, including LV dilation, wall thinning, and shape alterations and that this remodeling predicts overall morbidity and cardiovascular mortality.<sup>4</sup> Patient-specific LV geometry can now be analyzed with unprecedented accuracy, with recent advances in image-based data acquisition and analysis. On one hand, clinical cardiac magnetic resonance (CMR) imaging and its combination with late gadolinium enhancement can effectively and noninvasively acquire global indices of 3-dimensional (3D) LV structure in health and disease.<sup>1</sup> On the other hand, the new field of computational anatomy offers rigorous mathematical and algorithmic tools

This work was supported by National Institutes of Health grants R01HL103812 (to Dr Wu), R01HL103428 (to Dr Trayanova), and DP1HL123271 (to Dr Trayanova) as well as by American Heart Association grant 13SDG14510061 (to Dr Vadakkumpadan). **Address reprint requests and correspondence:** Dr Fijoy Vadakkumpadan, Department of Biomedical Engineering, Institute for Computational Medicine, Johns Hopkins University, 3400 N Charles St, Hackerman 217B, Baltimore, MD 21218. E-mail address: fijoy@jhu.edu.

for the detailed assessment of segmental differences in image-based cardiac geometry.<sup>5</sup> Leveraging these advances to incorporate regional metrics of LV remodeling may help identify patients at a higher vs lower risk of SCD. Ideally, an anatomical biomarker could also differentiate patients with a high risk of SCD from those who do not have SCD outcomes but instead eventually succumb to heart failure (HF), which is an important competing cause of death in patients with cardiomyopathy and for which the management approach can be quite different.

The overarching goal of our research is to uncover novel, image-based, 3D indices of LV geometry that can be used to predict SCD risk specifically. The present study is a proof of concept, in which we have implemented a framework that uses CMR, advanced image processing, and computational anatomy tools to compare 3D LV endocardial surface curvature, wall thickness (WT), and relative wall thickness (RWT) between patient groups. We have retrospectively applied our methodology to data from patients with ischemic cardiomyopathy who were selected for ICD implantation on the basis of reduced LVEF, followed by implantation for clinical events, and divided into groups with differing SCD risk on the basis of follow-up time. We hypothesized that 3D LV shape metrics could identify patients at the highest risk for SCD. We also explored whether shape metrics alone could differentiate between SCD and HF outcomes.

## Methods

Our framework is outlined in Figure 1, which shows how a patient heart image is processed with our pipeline, including reconstruction of 3D LV geometry, segmentation of endocardial surface, computation of 3D shape metrics, and regionwise statistical analysis. The data acquisition and the components of the pipeline are described in the following sections.

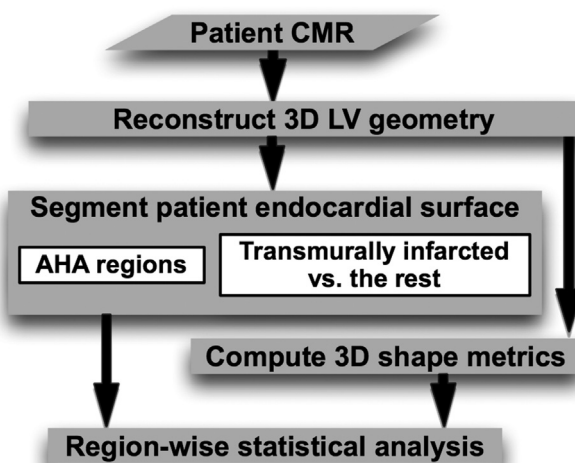


**Figure 1** The processing pipeline of our computational framework. 3D = 3-dimensional; AHA = American Heart Association; CMR = cardiac magnetic resonance; LV = left ventricular.

## Data acquisition

The data used for the present study consisted of late gadolinium-enhanced cardiac magnetic resonance images of 61 patients with ischemic cardiomyopathy and LVEF  $\leq 35\%$ , which represented a random sample from the CMR arm of the prospective observational study of implantable cardioverter-defibrillators at Johns Hopkins University.<sup>1</sup> In the CMR arm of the prospective observational study of implantable cardioverter-defibrillators, all patients were imaged, implanted with ICDs for the primary prevention of SCD, and then followed for events, including appropriate ICD firings, sudden arrhythmic death (SAD), and death or hospitalization due to HF. We divided the 61 patients into 3 groups: group 0 consisted of 28 patients with no events during follow-up, group 1 included 18 patients who either suffered from SAD or whose ICDs fired appropriately, and group 2 composed of 15 patients who died of or were hospitalized for HF, but did not have an arrhythmic event. Patients who had both an arrhythmic event and HF were included in group 1 (for more details, see [Section 1 in the Online Supplement](#)).

## Reconstruction of 3D LV geometry

In each short-axis slice of the image, the LV endocardium and epicardium were semiautomatically contoured. The septal part of the endocardial contour was then manually identified by placing 2 landmark points near the right ventricular insertion points ([Figure 2A](#)). Investigators who performed the contouring and landmark placement were blinded to the patient groups. From the contours and landmark points, 3 sets of 2-dimensional (2D) binary masks, each set implicitly representing the LV endocardium, LV epicardium, and septal endocardium were constructed ([Figure 2B](#)). Each set of 2D masks was then interpolated to build a 3D binary mask at 1 mm isotropic resolution.<sup>6</sup> Finally, the geometry image of the LV wall was generated by combining the three 3D masks ([Figure 2C](#)) (for more details, see [Section 2 in the Online Supplement](#)).

## Computation of shape metrics

For each image voxel along the endocardial surface, curvedness of the surface as well as WT and RWT of the LV were computed. Curvedness characterizes the deviation of a surface from flatness and is defined as the root mean square of principal curvatures.<sup>7</sup> We computed the principal curvatures as described in Goldman<sup>8</sup> from a Gaussian-smoothed version of the 3D mask for the LV chamber illustrated in [Figure 2C](#). The WT at an endocardial surface voxel was calculated as the distance to the nearest voxel that lied along the epicardium. The RWT at an endocardial surface voxel was computed as the product of curvedness and WT at that voxel ([Figure 3](#)). This definition of RWT is our 3D extension of a 2D echocardiographic concept,<sup>9</sup> where RWT is defined as the ratio of posterior or septal WT to radius of the LV endocardium in diastole. Since curvedness is the inverse of radius,<sup>7</sup> the product of curvedness and WT is a measure of RWT (for more details, see [Section 3 in the Online Supplement](#)).

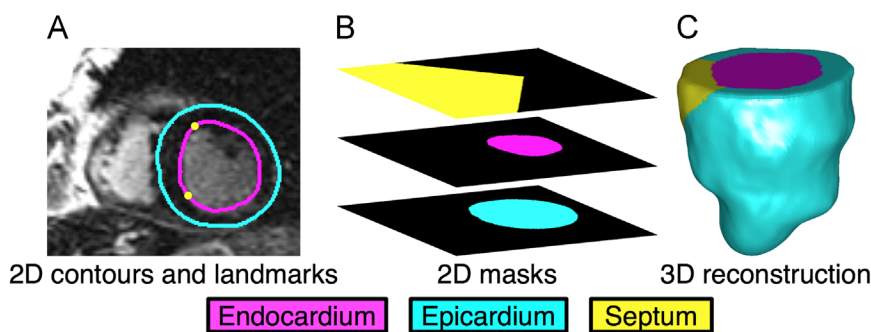


**Figure 2** Reconstruction of 3D LV geometry from CMR image slices. **A:** Example of slice with endocardial/epicardial contours and landmarks corresponding to the septum. **B:** The 2D endocardial, epicardial, and septal masks for the slice. **C:** The reconstructed 3D geometry in the anterior view. 2D = 2-dimensional; 3D = 3-dimensional; CMR = cardiac magnetic resonance; LV = left ventricular.

### Segmentation of the endocardial surface of the patient

To perform localized statistical analysis, the endocardial surface of each patient LV geometry was segmented on the basis of American Heart Association (AHA) myocardial regions<sup>10</sup> as well as local transmurality of the infarct (for details on the segmentation, see [Section 4 in the Online Supplement](#)). Briefly, to automate the segmentation into AHA regions, 1 LV geometry (referred to as the atlas) was selected and it semi-automatically segmented into the AHA regions.<sup>11</sup> This atlas was then deformed to match each of the remaining patient LV geometries using affine transformation and the computational anatomy algorithm termed multichannel large deformation diffeomorphic metric mapping.<sup>12</sup> These deformations provided, for each point in the atlas, the anatomically corresponding points on patient LV geometries. Finally, each voxel on the endocardial surface of a patient LV geometry was classified as belonging to the same AHA region as the anatomically corresponding point on the atlas ([Figures 4A–4D](#)).

To segment the endocardial surface of a patient LV into transmurally infarcted regions and the rest, first the infarct zone was planimetered on each short-axis 2D slice.<sup>1</sup> Second, a 3D reconstruction of the infarct geometry was obtained at 1 mm isotropic resolution by using a shape-based binary interpolation method.<sup>13</sup> Third, at each endocardial surface voxel  $v$ , a line

segment was computed by connecting  $v$  to the nearest epicardial surface voxel and the transmural extent of the infarct (TEI) at  $v$  was calculated as the proportion of this line segment that intersects with the 3D reconstruction of the infarct geometry. Finally, each endocardial surface voxel with  $\text{TEI} \geq 75\%$  was classified as transmurally infarcted ([Figures 4E–4G](#)). This particular threshold is often used to delineate transmural scar.<sup>14</sup>

### Statistical analyses

Baseline characteristics were summarized as means or proportions for each patient group and statistically compared between groups. The 3D distribution of TEI was derived by calculating, at each point  $p$  on the atlas endocardial surface, the mean and SD of TEIs at points on patient LVs that corresponded to  $p$  according to the deformations of the atlas geometry. Similarly, the distributions of the shape metrics were generated. The mean TEI in each of the 3 coronary arterial territories, namely, left anterior descending (LAD) artery, right coronary artery, and left circumflex artery, was calculated on the basis of the segmentation of the atlas endocardium into AHA regions and the correspondence between the AHA regions and the territories.<sup>10</sup> AHA region 17 was excluded from all analyses because of limited image resolution at the apex (see [Section 1 in the Online Supplement](#)). Differences in the mean TEI between groups and between coronary artery territories were examined. In each of the coronary artery regions of each patient, the mean of each shape metric was calculated as the average of the metric at all points in the region, and differences in the mean of the shape metrics between pairs of groups were assessed. For each patient group and for each coronary artery region, differences in mean of the shape metrics between transmurally infarcted areas and the rest were evaluated. In all statistical comparisons, correction for covariates was performed using linear regression and multiple comparison errors were eliminated using permutation tests (for more details, see [Section 5 in the Online Supplement](#)).

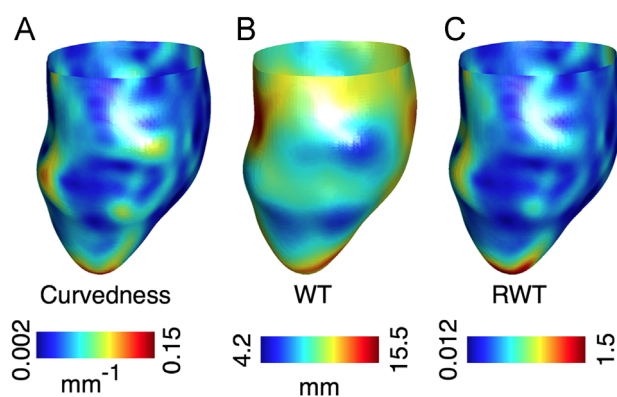


**Figure 3** Shape metrics computed for the LV geometry shown in [Figure 2C](#), displayed on the endocardial surface in the anterior view: (A) curvedness; (B) WT; (C) RWT. LV = left ventricular; RWT = relative wall thickness; WT = wall thickness.

## Results

### Baseline characteristics

The baseline characteristics of the patient cohort are summarized in [Table 1](#). The mean follow-up time for patients without events was  $8.4 \pm 0.7$  years. All characteristics were

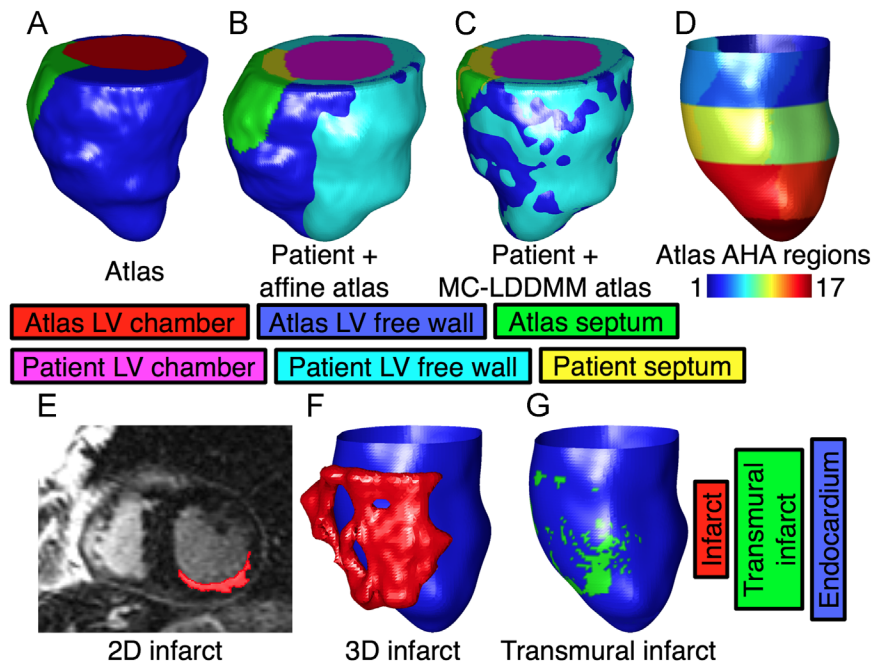


**Figure 4** Segmentation of endocardial surfaces of patients as described in the Methods section. **A:** Atlas geometry in the anterior view. **B:** Superimposition of the patient heart geometry shown in **Figure 2C** and atlas geometry after affine transformation. **C:** The patient heart geometry and the atlas geometry after MC-LDDMM transformation. **D:** Posterior view of the segmentation of the endocardial surface of the patient heart geometry into 17 AHA regions. **E:** Segmentation of the infarct region in an example of 2D slice of the patient. **F:** 3D reconstruction of the infarct region of the patient, along with the endocardial surface. **G:** Segmentation of the endocardial surface of the patient into transmurally infarcted regions and the rest. 2D = 2-dimensional; 3D = 3-dimensional; AHA = American Heart Association; LV = left ventricular; MC-LDDMM = multichannel large deformation diffeomorphic metric mapping.

statistically insignificant, but diabetes ( $P = .06$ ) was more prevalent in group 2 and CMR LVEF ( $P = .17$ ) trended lower in group 1. **Figure 5** shows the anterior view of the spatial distribution of TEI in the patient cohort as well as comparisons of the mean TEI between groups and between coronary artery

territories. The mean TEI in the LAD region was significantly higher in 4 comparisons. There was only 1 significant intergroup comparison, but in general, TEI did not differ between outcome groups. **Figure 5** also displays the spatial distributions of the shape metrics in the entire patient cohort.

**Table 1** Baseline characteristics of the patient cohort

Characteristic	Group 0 (no event; n = 28)	Group 1 (ICD firing or SAD; n = 18)	Group 2 (HF n = 15)	P
Sex: male	23 (82)	14 (78)	12 (80)	.97
Age (y)	61.9 ± 10.7	61.0 ± 10.8	63.3 ± 11.1	.89
White	23 (82)	16 (89)	12 (80)	.89
Years from infarction incidence/diagnosis	8.1 ± 7.2	8.8 ± 6.0	5.9 ± 6.8	.38
New York Heart Association functional class				.68
I	10 (36)	4 (22)	4 (27)	
II	9 (32)	9 (50)	4 (27)	
III	9 (32)	5 (28)	7 (46)	
Hypertension	23 (82)	11 (61)	11 (73)	.49
Hypercholesterolemia	23 (82)	13 (72)	11 (73)	.82
Diabetes	7 (25)	5 (28)	10 (67)	.06
Nicotine use	20 (71)	15 (83)	10 (66)	.68
Biventricular ICD	4 (14)	3 (17)	5 (33)	.57
Enrollment LVEF (non-CMR) (%)	25.8 ± 6.7	22.1 ± 7.6	23.7 ± 6.8	.27
CMR characteristics				
LVEF (%)	30.0 ± 7.4	24.5 ± 9.0	29.2 ± 8.8	.17
LV end-diastolic volume (mL)	236.9 ± 67.0	238.1 ± 89.0	226.0 ± 63.4	.90
LV end-systolic volume (mL)	166.8 ± 55.3	181.8 ± 74.4	163.6 ± 62.4	.74
LV mass (g)	189.3 ± 53.4	168.1 ± 46.5	175.5 ± 55.0	.41
Total infarct mass (LGE-CMR) (g)	36.6 ± 17.8	38.9 ± 18.7	38.8 ± 36.6	.62

Data are presented as mean ± SD or n (%).

HF = heart failure; ICD = implantable cardioverter-defibrillator; LGE-CMR = late gadolinium-enhanced cardiac magnetic resonance; LV = left ventricular; LVEF = left ventricular ejection fraction; SAD = sudden arrhythmic death.

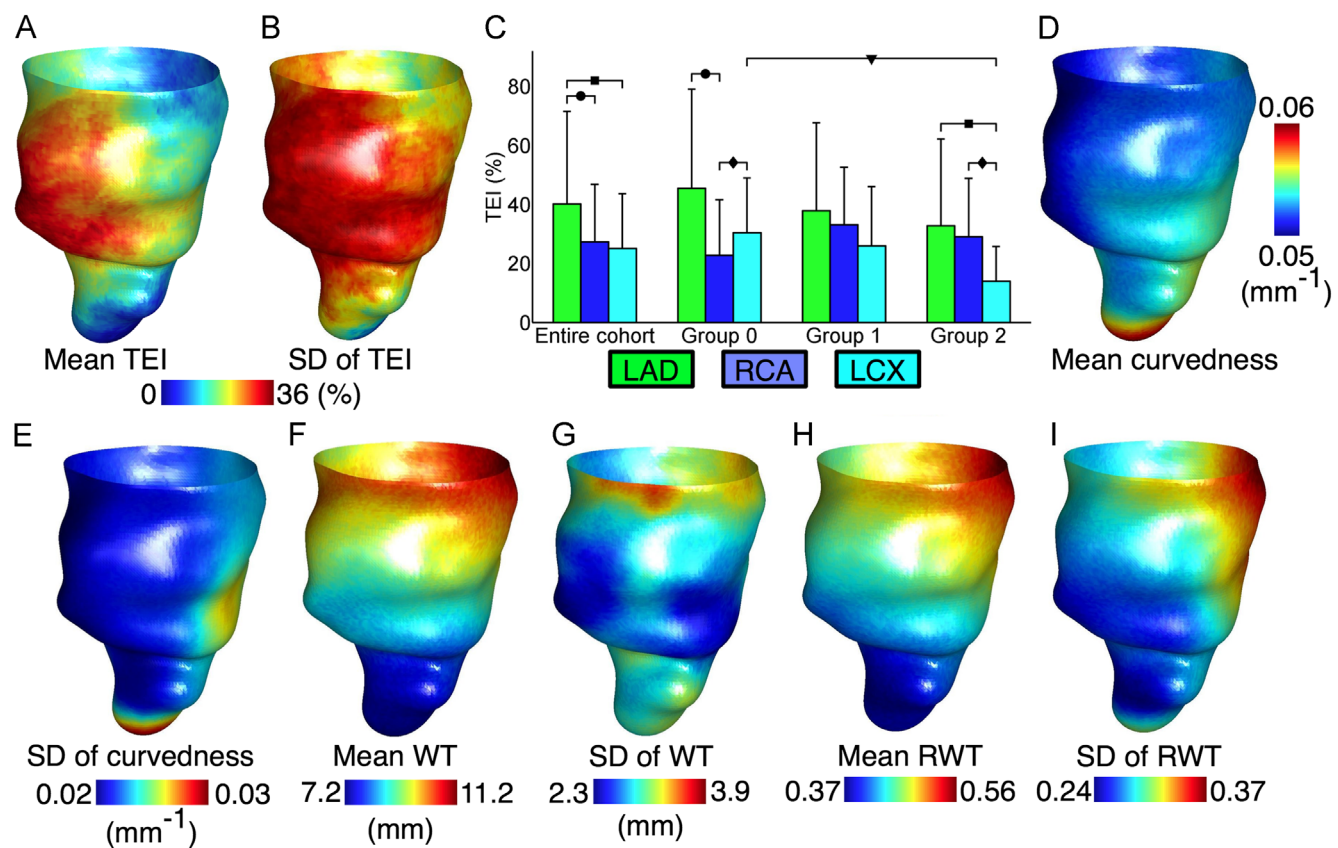


**Figure 5** Distributions of the TEI and the shape metrics. **A and B:** The mean and SD, respectively, of the TEI in the entire patient cohort, at each point on the 3D atlas endocardial surface in the anterior view. **C:** The mean and SD of the transmural extent in the entire cohort and each of the patient groups in each of the coronary artery territories. Brackets with different symbols indicate significant differences between patient groups for the same coronary artery region and between coronary artery regions for the same group. **D, F, and H:** The mean of curvedness, WT, and RWT, respectively, in the entire patient cohort at each point on the atlas endocardial surface in the anterior view. **E, G, and I:** The SD of curvedness, WT, and RWT, respectively, over the atlas endocardial surface. 3D = 3-dimensional; LAD = left anterior descending; LCX = left circumflex artery; RCA = right coronary artery; RWT = relative wall thickness; TEI = transmural extent of the infarct; WT = wall thickness.

### Shape differences between outcome groups within coronary artery regions

Figure 6 shows a comparison of the shape metrics between groups in each of the coronary artery regions. In all regions, groups with an event had lower mean curvedness, WT, and RWT. Of the 27 intergroup comparisons, 9 were statistically significant. Among the 3 shape metrics, the maximum number of significant differences was found in RWT. There were no significant differences in the shape metrics between groups 1 and 2.

### Shape differences within outcome groups between transmurally infarcted and the remaining regions

Within each patient outcome group and within each coronary artery subdivision, Figure 7 shows comparisons of the shape metrics between transmurally infarcted regions and either nontransmurally infarcted or normal regions. In all but 4 comparisons and in all significant comparisons, the shape metrics were lower in transmurally infarcted areas. Four of the 8 significant comparisons involved the LAD coronary artery territory, reflecting increased LV remodeling in this territory owing to transmural infarction.

### Discussion

This research aimed to investigate whether image-based 3D regional indices of LV geometry can differentially identify SCD risk. To this end, we implemented a proof-of-concept framework which is novel in that it combines CMR and computational anatomy. We applied the methodology to a cohort of patients with ischemic cardiomyopathy and LV dysfunction and revealed, for the first time, that differences in local 3D LV endocardial curvedness, WT, and RWT can be identified between those with no events during clinical follow-up and those with arrhythmic or HF events, despite similar global indices of remodeling (LV volumes and mass). Our results also suggest that the LV anatomical substrate may be similar in patients who are susceptible to either ventricular arrhythmias or HF. Hence, LV anatomical parameters alone may not be able to definitively differentiate between the 2 competing causes of death in patients with cardiomyopathy, that is, SAD and pump failure. Nonetheless, incorporating the proposed shape metrics into SCD risk prediction has the potential to help enhance the accuracy of image-based risk stratification approaches by accounting for individual differences in regional LV anatomy that are not adequately described by the currently used global LV metrics.

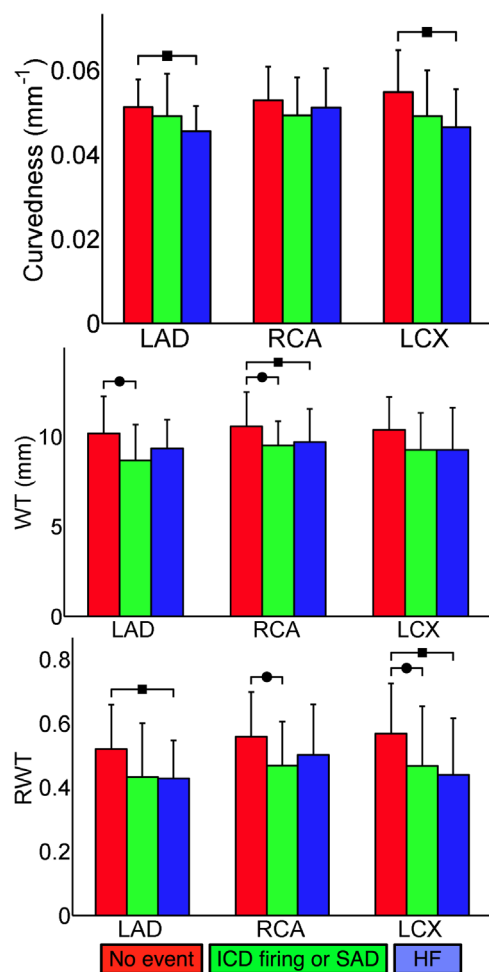


**Figure 6** Between group analysis: mean and SD of curvedness, WT, and RWT between each of the patient groups and for each of the coronary artery regions. Brackets with different symbols indicate significant differences. HF = heart failure; ICD = implantable cardioverter-defibrillator; LAD = left anterior descending; LCX = left circumflex artery; RCA = right coronary artery; RWT = relative wall thickness; SAD = sudden arrhythmic death; WT = wall thickness.

and by identifying a cohort with favorable LV anatomy that portends good prognosis.

Previous studies have shown that global LV volume and mass are associated with a composite of cardiovascular events postinfarction.<sup>9</sup> In addition, it is known that global LV shape, as measured in 2D approaches by the so-called sphericity index, can predict adverse clinical outcomes, including cardiovascular death and HF, even after controlling for LV volumes.<sup>15,16</sup> Also, categorization of LV geometry into 4 classes on the basis of LV mass index and RWT measured from 2D or M-mode echocardiograms has recently been found to be associated with cardiovascular risk.<sup>9</sup> Despite the numerous efforts to correlate indices of LV remodeling with clinical outcomes, it remains unknown whether these indices, especially those that characterize LV shape, can be useful in predicting SCD risk. Furthermore, the LV shape indices in existing studies are restricted to 2D global measurements. Qualitatively, since the same 2D global measurement can correspond to any number of

3D shapes, as in the example of the 2D sphericity index, the discriminability of 2D indices is poor.<sup>17</sup> In the present study, we have developed a state-of-the-art computational framework to statistically compare 3D indices of regional LV shape between patient groups and used this framework to demonstrate differences between patients with a low risk of SCD and those with a high risk of SCD. A further quantitative comparison of global 2D and regional 3D metrics is needed to conclusively demonstrate the superiority of the latter.

Our patient cohort was fairly typical of others with ischemic cardiomyopathy.<sup>18</sup> There was a predominance of scar involving the LAD distribution, with a lesser prevalence of scar in the right coronary artery and left circumflex artery territories. The magnitude of LV curvedness and WT values in the present study are comparable to those published elsewhere for patients with ischemic cardiomyopathy.<sup>7,11</sup> In addition, it is clear from Figure 5 that as one proceeds from the base to apical portions of the LV, the curvedness increases and WT decreases, as expected.<sup>19,20</sup> Incidentally, only computational anatomy techniques such as the ones we use in this study can generate the 3D distributions in Figure 5. Our results are consistent with previous studies which showed that global LV dilation and wall thinning postinfarction correlate with adverse cardiovascular events.<sup>4</sup> Furthermore, our study provides novel findings in demonstrating that the differences in curvedness, WT, and RWT exist locally throughout the LV as well as between patients without events and those with specifically arrhythmic or HF events. Notably, it remains unknown whether LV shape analysis can be used to differentiate patients with arrhythmic events and those with HF events, as our study revealed no significant differences between these 2 groups. Similar LV shape changes can predispose patients to both ventricular arrhythmias and HF complications owing to heterogeneity in LV mechanics, but for clinical management, one would ideally be able to differentiate the 2. Our results suggest that LV shape metrics alone may be insufficient for this purpose, and future studies could combine other biomarkers with LV shape indices. Nonetheless, our findings remain important in that 3D shape analysis was able to differentiate patients without events from those with events. Hence, one may be able to improve identification of the low-risk population by the lack of significant regional LV remodeling in 3D shape analysis. Those patients who do have significant regional LV remodeling may benefit from more aggressive HF therapies as well as prophylactic ICDs. Our results in Figure 7 demonstrate that the shape metrics were lower in transmurally infarcted areas and the most pronounced differences occurred in the LAD territory. This corroborates existing evidence indicating that transmurally infarcted regions expand, and this occurs more commonly in the anterior, anteroseptal, and anteroapical regions.<sup>21,22</sup>

Mechanistically, it has been postulated that LV dilation and wall thinning, similarly to those illustrated in Figure 6, lead to worse arrhythmic outcomes because of increased wall strain and stress, which in turn trigger stretch-activated ion

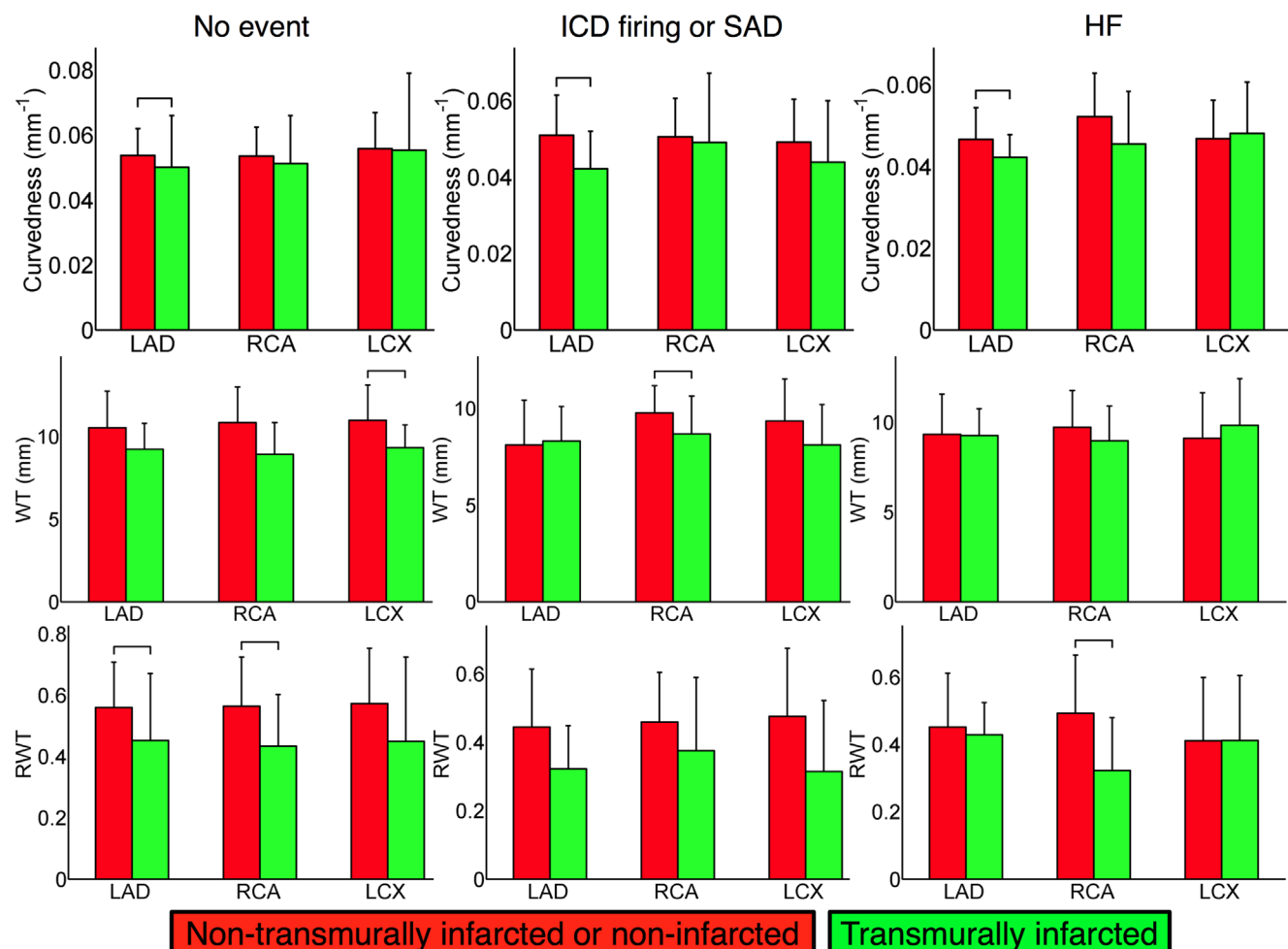


**Figure 7** Within group analysis: mean and SD of the shape metrics in the nontransmurally infarcted or normal and transmurally infarcted regions, in each of the coronary artery, within each patient group (columns). Brackets indicate significant differences. HF = heart failure; ICD = implantable cardioverter-defibrillator; LAD = left anterior descending; LCX = left circumflex artery; RCA = right coronary artery; RWT = relative wall thickness; SAD = sudden arrhythmic death; WT = wall thickness.

channels.<sup>23,24</sup> Also, LV remodeling is correlated with infarct size,<sup>25,26</sup> and so are arrhythmic events.<sup>27</sup> The increased wall stress caused by LV dilation and thinning also elicit compensatory responses, and when these responses are inadequate, a vicious cycle of further dilation ensues and the heart eventually fails.<sup>25,28</sup> Note that increases in wall stress are believed to be the principal change that occurs during LV remodeling,<sup>4</sup> and our RWT metric accounts for both radius of curvature and WT, the 2 geometric parameters that contribute to wall stress.<sup>29</sup> Hence, of the 3 shape metrics we considered in this study, RWT produced the maximum number of significant differences between patients with events and those without events.

The novel computational framework and findings in this study constitute an important step toward the use of LV shape indices in the clinical risk stratification of patients with cardiomyopathy. We envision that the shape indices we propose could potentially be used in combination with existing predictors of SCD such as LV and scar volumes to train a statistical model, which, given the shape metrics of a patient, may noninvasively and reliably compute a personalized risk

score that reflects the patient's susceptibility to SCD. The framework that we have developed is equally applicable to patients with nonischemic etiologies or with LVEF  $\geq 35\%$  and can incorporate any pointwise shape metric. Similarly, our methodology can be straightforwardly extended to use other clinical imaging modalities such as cine magnetic resonance imaging sequences or cardiac computed tomography.

A limitation of the present methodology is that the contouring of endo- and epicardial boundaries requires significant manual intervention, which is time-consuming. Planimetry techniques that are more automated<sup>30</sup> may be incorporated into our framework. The lack of statistical significance in some intergroup comparisons is a drawback of our results. However, we show that groups with events have lower shape metrics in all comparisons, and it is expected that some of the nonsignificant comparisons will become significant as the sample size is increased. Also, only end-diastolic images are used in this study. Our framework can be extended to use the end-systolic phase, where the effects of LV remodeling are more pronounced,<sup>7,29</sup> and to analyze change in shape metrics over the cardiac cycle.

## Conclusion

We have developed a novel methodology that uses CMR and computational anatomy tools to detect regional differences in 3D LV shape between patient groups. By using this methodology, we showed that, in patients with ischemic cardiomyopathy and low LVEF, there exist differences in LV endocardial curvedness, WT, and RWT between those with no clinical events and those who develop arrhythmic or HF events. This retrospective study is a proof of concept supporting additional research to investigate the use of LV shape metrics, likely in combination with other risk markers, to improve SCD risk stratification and potentially guide treatment delivery.

## Appendix

### Supplementary data

Supplementary data associated with this article can be found in the online version at <http://dx.doi.org/10.1016/j.hrthm.2014.05.018>.

## References

1. Wu KC, Gerstenblith G, Guallar E, Marine JE, Dalal D, Cheng A, Marbán E, Lima JAC, Tomaselli GF, Weiss RG. Combined cardiac MRI and C-reactive protein levels identify a cohort at low risk for defibrillator firings and death. *Circ Cardiovasc Imaging* 2012;5:178–186.
2. Santangeli P, Russo AD, Casella M, Pelargonio G, Di-Biase L, Natale A. Left ventricular ejection fraction for the risk stratification of sudden cardiac death: friend or foe? *Intern Med J* 2011;41:55–60.
3. Lopera G, Curtis A. Risk stratification for sudden cardiac death: current approaches and predictive value. *Curr Cardiol Rev* 2009;5:56–64.
4. Mann DL, Bristow MR. Mechanisms and models in heart failure: the biomechanical model and beyond. *Circulation* 2004;111:2837–2849.
5. Beg MF, Helm PA, McVeigh E, Miller MI, Winslow RL. Computational cardiac anatomy using MRI. *Magn Reson Med* 2004;52:1167–1174.
6. Turk G, O'Brien J. Shape transformation using variational implicit functions. In: Proc SIGGRAPH '99: Proceedings of the 26th Annual Conference on Computer Graphics and Interactive Techniques. New York: ACM Press/Addison-Wesley Publishing Co; 1999:335–342.
7. Zhong L, Su Y, Yeo S-Y, Tan R-S, Ghista DN, Kassab G. Left ventricular regional wall curvedness and wall stress in patients with ischemic dilated cardiomyopathy. *Am J Physiol Heart Circ Physiol* 2009;296:H573–H584.
8. Goldman R. Curvature formulas for implicit curves and surfaces. *Comput Aided Geom Des* 2005;22:632–658.
9. Konstam MA, Kramer DG, Patel AR, Maron MS, Udelson JE. Left ventricular remodeling in heart failure: current concepts in clinical significance and assessment. *JACC Cardiovasc Imaging* 2011;4:98–108.
10. Cerqueira MD, Weissman NJ, Dilsizian V, Jacobs AK, Kaul S, Laskey WK, Pennell DJ, Rumberger JA, Ryan T, Verani MS. Standardized myocardial segmentation and nomenclature for tomographic imaging of the heart: a statement for healthcare professionals from the Cardiac Imaging Committee of the Council on Clinical Cardiology of the American Heart Association. *Circulation* 2002;105:539–542.
11. Su Y, Zhong L, Lima C-W, Ghistac D, Chua T, Tan R-S. A geometrical approach for evaluating left ventricular remodeling in myocardial infarct patients. *Comput Methods Progr Biomed* 2012;108:500–510.
12. Ceritoglu C, Oishi K, Li X, Chou MC, Younes L, Albert M, Lyketsos C, van Zijl PC, Miller MI, Mori S. Multi-contrast large deformation diffeomorphic metric mapping for diffusion tensor imaging. *Neuroimage* 2009;47:618–627.
13. Raya SP, Udupa JK. Shape-based interpolation of multidimensional objects. *IEEE Trans Med Imaging* 1990;9:32–42.
14. Boyé P, Abdel-Aty H, Zacharowsky U, Bohl S, Schwenke C, van der Geest RJ, Dietz R, Schirewan A, Schulz-Menger J. Prediction of life-threatening arrhythmic events in patients with chronic myocardial infarction by contrast-enhanced CMR. *JACC Cardiovasc Imaging* 2011;4:871–879.
15. Sutton MSJ, Plappert T, Rahmouni H. Assessment of left ventricular systolic function by echocardiography. *Heart Fail Clin* 2009;5:177–190.
16. Wong SP, French JK, Lydon AM, Manda SO, Gao W, Ashton NG, White HD. Relation of left ventricular sphericity to 10-year survival after acute myocardial infarction. *Am J Cardiol* 2004;94:1270–1275.
17. Salgo I, Tsang W, Ackerman W, Ahmad H, Chandra S, Cardinale M, Lang R. Geometric assessment of regional left ventricular remodeling by three-dimensional echocardiographic shape analysis correlates with left ventricular function. *J Am Soc Echocardiogr* 2012;25:80–88.
18. Rott D, Nowatzky J, Weiss AT, Chajek-Shaul T, Leibowitz D. ST deviation pattern and infarct related artery in acute myocardial infarction. *Clin Cardiol* 2009;32:E29–E32.
19. Maffessanti F, Lang R, Niel J, Steringer-Mascherbauer R, Caiani E, Nesser H, Mor-Avi V. Three-dimensional analysis of regional left ventricular endocardial curvature from cardiac magnetic resonance images. *Magn Reson Imaging* 2011;29:516–524.
20. Ho SY. Anatomy and myoarchitecture of the left ventricular wall in normal and in disease. *Eur J Echocardiogr* 2009;10:ii3–ii7.
21. McKay R, Pfeffer M, Pasternak R, Markis J, Come P, Nakao S, Alderman J, Ferguson J, Safian R, Grossman W. Left ventricular remodeling after myocardial infarction: a corollary to infarct expansion. *Circulation* 1986;74:693–702.
22. Weisman HF, Healy B. Myocardial infarct expansion, infarct extension, and reinfarction: pathophysiologic concepts. *Progr Cardiovasc Dis* 1987;30:73–110.
23. Miura M, Wakayama Y, Endoh H, Nakano M, Sugai Y, Hirose M, Keurs HET, Shimokawa H. Spatial non-uniformity of excitation-contraction coupling can enhance arrhythmic-delayed afterdepolarizations in rat cardiac muscle. *Cardiovasc Res* 2008;80:55–61.
24. Søgaard P, Götzsche CO, Ravkilde J, Nørgaard A, Thygesen K. Ventricular arrhythmias in the acute and chronic phases after acute myocardial infarction: effect of intervention with captopril. *Circulation* 1994;90:101–107.
25. Gaudron P, Eilles C, Kugler I, Ertl G. Progressive left ventricular dysfunction and remodeling after myocardial infarction: potential mechanisms and early predictors. *Circulation* 1993;87:755–763.
26. Cohn JN, Ferrari R, Sharpe N. Cardiac remodeling—concepts and clinical implications: a consensus paper from an international forum on cardiac remodeling. *J Am Coll Cardiol* 2000;35:569–582.
27. Schmidt A, Azevedo CF, Cheng A, Gupta SN, Bluemke DA, Foo TK, Gerstenblith G, Weiss RG, Marban E, Tomaselli GF, Lima JA, Wu KC. Infarct tissue heterogeneity by magnetic resonance imaging identifies enhanced cardiac arrhythmia susceptibility in patients with left ventricular dysfunction. *Circulation* 2007;115:2006–2014.
28. Vannan M, Taylor D. Ventricular remodelling after myocardial infarction. *Br Heart J* 1992;68:257–259.
29. Zhong L, Su Y, Gobeaowan L, Sola S, Tan RS, Navia JL, Ghista DN, Chua T, Guccione J, Kassab GS. Impact of surgical ventricular restoration on ventricular shape, wall stress, and function in heart failure patients. *Am J Physiol Heart Circ Physiol* 2011;300:H1653–H1660.
30. Petitjean C, Dacher JN. A review of segmentation methods in short axis cardiac MR images. *Med Image Anal* 2011;15:169–184.